Cone Penetration Testing 2022 – Gottardi & Tonni (eds)

Liquefaction damage assessment using Bayesian belief networks

L. Paolella, A. Baris & G. Modoni
University of Cassino and Southern Latium, Italy

R.L. Spacagna & S. Fabozzi
CNR IGAG, Area della Ricerca Roma 1, Italy

ABSTRACT: The seismic and liquefaction risk assessment implies introducing methods based on different hypotheses and dealing with different levels of uncertainty affecting the whole process from triggering to surficial manifestation. In this context, soft computing methods, like Bayesian Belief Networks (BBN) and artificial intelligence algorithms, provide the logic framework for cause-effect relationships and the statistical statement to manage uncertainties. Taking advantage of the significant amount of geotechnical data and post-earthquake surveys, an application of BBN versus the forecasting of liquefaction-induced ground damage is proposed considering three main shocks of the 2010 – 2011 Christchurch (New Zealand) Earthquakes Sequence. The BBN algorithms are firstly employed to identify significant variables and learn the relationships among them, then a direct and graphical link between input and target data is created. The quantitative validation of the built architecture enables to advantageously queried the net to predict the result of new datasets.

1 INTRODUCTION

The chain phenomena describing the liquefaction process involve numerous and complex relationships that rule the origin, propagation, surficial manifestation, and induced structural and infrastructural damage. In the field of Earthquake Engineering, the cause-effect relationships starting from the probability of occurrence of a predefined intensity measure have been translated into the PEER convolutive integral (Cornell and Krawinkler, 2000), which develops the performance-based earthquake engineering approach.

In recent years, the development of soft computing methods and the progress in artificial intelligence A.I. provide robust and reliable instruments capable of dealing with large amounts of data in a reasonable time, controlling the quality of results and quantifying uncertainties. Artificial Neural Networks (ANNs) and Bayesian Belief Networks (BBNs) have been advantageously used in various engineering applications to identify the most significant variables, learn the relationships and dependencies among them, and link the input data to the target. After scrutinizing the new data collection campaigns following the 2012 Emilia (Italy) Earthquake sequence, Paolella et al. (2019) developed artificial neural networks and Monte Carlo simulations to relate the Ishihara-based geotechnical model to the observed ground liquefaction in the municipality of San Carlo. Ching and Phoon (2017) developed a method based on the sparse Bayesian learning (SBL) approach to analyze site-specific measurements like cone penetration test (CPT) data for probabilistic site characterization. A detailed study has been carried out by Tesfamariam (2013) about liquefaction risk that calibrates four different BBN structures and defines a procedure to assess the liquefaction risk at the regional and single building levels. Tang et al. (2018) compare ANN technology and BNNs in describing the liquefaction ground severity demonstrating that the Bayesian model achieves better accuracy for each damage state. Taking advances from previous experiences and the considerable amount of geotechnical data, a BN model for liquefaction prediction is proposed in this work. The best structure is obtained after the processing of ≈9′000 CPTs available from the New Zealand Geotechnical Database and testing each performance against three main events of the 2010-2011 Canterbury Earthquake Sequence. In a preliminary analysis, the back analysis enables the reconnaissance of the critical layer, *i.e.,* the sandy stratum most likely to undergo liquefaction during the 2010-2011 Christchurch earthquake sequence. The obtained results have shown that, if opportunely guided, the model can relate pre-defined representative variables to liquefaction ground evidence, the latter available from specific post-earthquake surveys. In a subsequent step, more detailed evaluations have been performed on such a critical layer, and a set of site-specific soil fragility functions is proposed. Uncertainties at different levels are accounted for through statistical and probabilistic terms, displaying

DOI: 10.1201/9781003308829-156

and controlling each variable. In conclusion, an alternative approach to large areas studies (Spacagna et al., 2021) and traditional liquefaction severity indicators often evaluated deterministically is presented by developing a set of fragility functions.

2 BAYESIAN BELIEF NETWORKS

A Bayesian Network falls in the category of probabilistic graphical modeling (PGM) technique that is to compute uncertainties by using the probability concept (Pearl, 1988). It is represented as a directed acyclic graph (DAG) which contains a set of nodes and links, arches, relating parent nodes to the children ones. A directed acyclic graph evaluates the uncertainty of an event occurring based on the conditional probability distribution of each random variable. A conditional probability table is used to represent this distribution of each variable in the network.

To understand the meaning, it is necessary to introduce the inference algorithm that is based on the Bayes theorem and conditional independence as follows:

$$P(B|A) = \frac{P(\mathrm{A}|\mathrm{B})P(B)}{P(A)} \quad (1)$$

It introduces joint probability, a measure of two events happening simultaneously *i.e., P(A|B)*, and the conditional probability of an event B, which is the probability that event B occurs given that an event A has already occurred. The Bayesian Networks satisfy the Local Markov Property, stating that a node is conditionally independent of its non-descendants, given its parents. In the example of Figure 1, *P(D|A, B)* is equal to *P(D|A)* because D is independent of its non-descendent, B. This property aids us in simplifying the Joint Distribution. The Local Markov Property leads us to the concept of a Markov Random Field, which is a random field around a variable that is said to follow Markov properties.

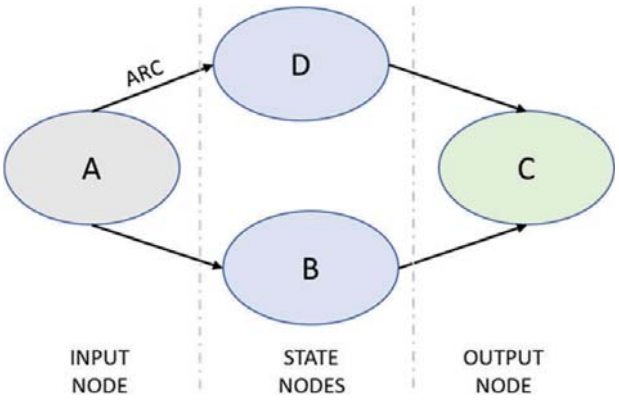

Figure 1. Scheme of a sample Bayesian Network.

Proven that the probability of a random variable depends on his parents, a Bayesian Network can be generalized as shown in Eqn. 2:

$$P(X_1, .., X_n) = \prod_{i=1}^{n} p(X_i|Parents\,(X_i)) \quad (2)$$

2.1 *Bayesian Networks for liquefaction hazard*

In general, the assessment of liquefaction hazard moves from subsequent steps, which translate the soil propensity to liquefy, the triggering analysis, and the liquefaction-induced ground deformation (Bird et al., 2005). Therefore, a BN model for liquefaction hazard requires introducing three types of nodes: 1) input nodes that include soil parameters (e.g., relative density, plasticity, fine contents), site conditions (groundwater depth, thickness and position homogeneous layers, distance from geological features like rivers/paleochannels) and seismic intensity measures (peak ground acceleration, Magnitude, duration, epicentral distance); 2) state nodes which combine input into intermediate variables (*i.e.,* the classification of soil susceptibility, the probability of triggering the phenomenon), and 3) output nodes describing the severity of liquefaction-induced ground observations.

Hu et al. (2016) provided an example of a net that constructed a model for liquefaction potential evaluation considering 12 factors. In this study, a revised approach is proposed, to link geotechnical and geological susceptibility to free field liquefaction ground evidence via the Arias Intensity, without evaluating traditional liquefaction severity indicators, *i.e.,* simplifying an intermediate step that unavoidably introduces noises.

After selecting representative variables for liquefaction, several net models are automatically generated and tested. With this regard, updating the net calculates the probability of having a particular combination of input variables given the evidence, allowing to determine the size, position, and strength characterization of the most likely layer experiencing liquefaction during the considered Earthquake sequence. On this layer, more detailed studies are carried out. The development of a probability model for liquefaction occurrence considers different crust thickness, *Hc*, thick, *Hl*, and average resistance, mean *crr*, of the potentially liquefiable layer. The maximum likelihood criterion is applied to fit the histograms data to lognormal functions (Baker, 2013).

2.2 *Management of uncertainty and Validation*

Among the advantages of the proposed method there, is an immediate and reliable graphic tool that displays input variables and their relationships. Uncertainties in data estimates and the validity of basic assumptions (like the three-layer hypothesis) can be managed at different levels. In addition, the probabilistic model

allows practitioners to make predictions for future situations with a certain level of confidence. Validation criteria are required to assess the reliability of the obtained results. The metrics used in this study are borrowed from the binary validation methods Lusted (1971), which introduces the concept of Receiver Operative Characteristic Curves obtained by combining specificity and sensitivity; the Area Under the Curve (AUC) is a global proxy of the estimate quality. In addition, the Kappa statistics method is used to assess the agreement between the actual and expected results (Witten and Frank, 2005). Kappa statistics is defined in Equation 3: *Pa* is the fraction of agreement and *Pe* is the fraction of random agreement used to correct for values. *Pa* is a summation of the diagonal values of the confusion matrix.

$$K = \frac{Pa - Pe}{1 - Pe} \tag{3}$$

3 THE CASE STUDY OF CHRISTCHURCH (NEW ZEALAND)

3.1 *The 2010-2011 Canterbury Earthquake Sequence*

The city of Christchurch (≈370′000 inhabitants in 2011), in the Canterbury Region of the South Island of New Zealand, was repeatedly struck by earthquakes during the 2010-2011 seismic sequence known as Christchurch Earthquake Sequence (C.E.S) The most noticeable were: the Mw 7.1 Darfield event of September 4th 2010, the (Mw 6.2) Christchurch Earthquake of February 22nd 2011, resulting in 185 fatalities and diffuse devastation to dwellings and infrastructures and the Mw 6.0 June 13th 2011. Liquefaction played a significant role in causing the removal of 900′000 tons of liquefied soil, the demolition of 8′000 buildings (Cubrinovski, 2013; Tonkin & Taylor, 2013), and an economic loss of NZ$30 billion only on the residential sector (NZ Parliament).

3.2 *Creation of databases and variables management*

Taking advantage of the significant amount of geotechnical data, a general framework to develop BBN is developed. The strategy to reach such goals include: i) database construction and preliminary processing of CPT data; ii) sensitivity and correlation analyses; iii) automated training of different nets and validation test. In addition, a probabilistic model is derived from the output of the structure showing the best performance.

The database creation includes the collection and homogenization into a standardized format of many CPTs from the New Zealand Geotechnical Database. Out of 30′000 stratigraphies available on the whole Christchurch area, around 9′000 CPT profiles with a depth greater than 10m have been considered. In a preliminary phase, the Equivalent Soil Profile (ESP) method defined by Millen et al. (2020) is applied to determine the liquefaction susceptibility. This criterion converts a CPT profile into a three-layered equivalent one, defined by *Hc*, *Hl* and *crr* of the potentially liquefiable layer, with an error term used to confirm the consistency with the hypothesis of three-layered profile. The following analysis include three variables (*i.e.,* crust thickness, liquefiable thickness, and resistance), which define 22 homogeneous soil classes for liquefaction susceptibility taken from Millen et al. (2020) criterion. The groundwater table is not explicitly accounted since it is already considered in evaluating the crust thickness. In addition, the ESP normed error representing a check factor for the consistency with the 3-layered profile hypothesis is considered. On the other hand, the distance from riverbeds is assumed as a proxy for geological susceptibility. Seismic hazard is characterized for three earthquakes among the main events of the 2010-2011 C.E.S., *i.e.,* the Sept 2010 Mw7.1 Darfield earthquake, the Mw6.2 Feb 2011, and the Mw6.0 Jun 2011 Christchurch Earthquakes. For each of them, the Arias Intensity is evaluated elaborating the records of Central Christchurch strong motion stations. These scenarios are modeled through the fault distance and the Arias Intensity selected in place of the pair PGA-magnitude since it embeds the intensity and duration of the shaking. On the other hand, the liquefaction ground observation is classified as "YES" and "NO". The subsequent diagnostic inference showing the correlation between each variable and the observed liquefaction is reported in Figure 2. Just as an example of traditional severity indices, the van Ballegooy et al. (2014) Liquefaction Severity Number (LSN) which combines triggering with a hyperbolic weight function, is presented in Figure 2.

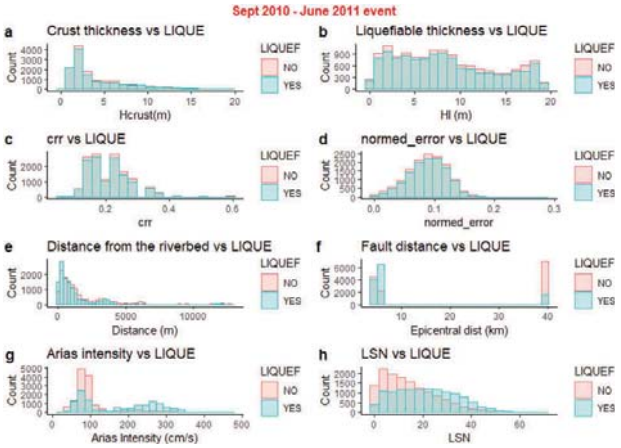

Figure 2. Sensitivity analysis of selected variables versus liquefaction ground observations: a) non-liquefiable crust thickness (m); b) thick of potentially liquefiable layer (m); c) mean crr; d) normed error (Millen er al., 2020); e) distance of investigated profile from riverbeds (m); e) epicentral distance (km); g) Arias (1970) Intensity (cm/s); h) LSN (van Ballegooy et al., 2014).

Although each variable of Millen et al. (2020) method seems to correlate to liquefaction poorly, if considered alone, from Figure 2, it is intuitive to observe that liquefaction occurrence increases with proportionally with the seismic shaking (see Arias Intensity) and close to riverbeds. The herein analyzed seismic scenarios remark that the relationship between seismic moment magnitude Mw and observed liquefaction is here strongly affected by the epicentral distance that made the Mw6.0 (located at approximately 5km from the City Center) and Mw6.2 February event, whose epicenter was around 6-7km South of Christchurch, more severe than the Mw7.1 Darfield event (epicenter 45km West of Christchurch).

In the following analysis, the existing dependencies among input variables are evaluated by calculating the Pearson coefficient; the resulting correlation matrix is plotted in Figure 3, whose coefficient font size is proportional to the correlation found. The massive amount of raw data, the lack of a predefined standard in the format, in conjunction with a certain level of subjectivity connected to post-earthquake rapid surveys, results in a non-negligible noise affecting the whole dataset. Therefore, Figure 3 shows a partial moderate/strong correlation between parameters introduced to quantify liquefaction susceptibility, which can be merged into one variable (*i.e.,* the ESP soil class) and between Arias Intensity and liquefaction severity indicators like LSN. However, to reduce the intermediate steps resulting in error, in the following process Arias Intensity is directly assumed as Engineering Demand Parameter for a given soil configuration, providing an alternative approach to traditional liquefaction severity indicators. In addition, the preliminary classification of variables applied by Millen et al. (2020) has been increased to investigate other geometric configurations better.

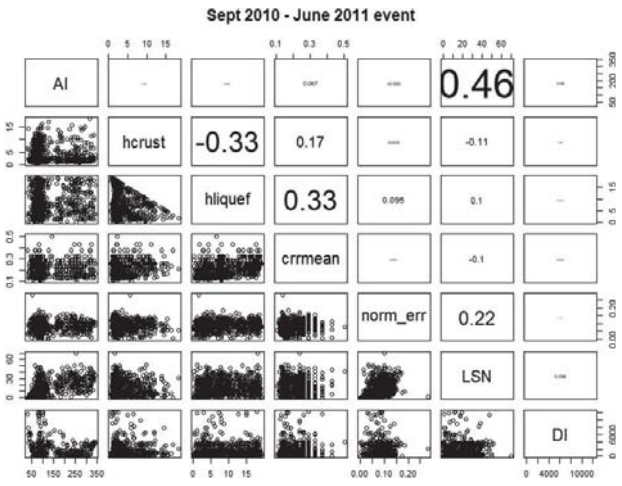

Figure 3. Correlation matrix of the considered variables for liquefaction.

3.3 *Training and validation of Bayesian Belief Networks for liquefaction*

To generate a BBN for liquefaction assessment, the local score metrics are considered for structure learning. Following the typical steps in assessing the liquefaction-induced permanent ground deformation, seven structures of Bayesian Belief Networks are trained and tested comparing the performance versus the liquefaction prediction capability for the Sept 2010 Mw7.1 Darfield earthquake, the Mw6.2 Feb 2011, and the Mw6.0 Jun 2011 Christchurch Earthquakes. Bearing in mind the results displayed in Figure 3, these networks architecture is built in the "Genie Academy" environment (Genie, 2020 https://www.bayesfusion.com/) by introducing different search algorithms. PC (Spirtes et al., 1993) uses independences observed in data (established employing classical independence tests) to infer the structure that has generated them and is the most adequate for continuous datasets; Naive Bayes and its improved version, *i.e.*, Tree Augmented Naïve Bayes (TAN) and Augmented Naïve Bayes (ANB), Bayesian search (BS), and Greedy thick thinning (GTT), respectively defined by Cooper and Herkovits (1992), and Cheng et al. (1997). Additionally, a background knowledge is provided to the PC algorithm to build an expert-guided network based on engineering judgment. The expert-guided model is displayed in Figure 4. The net is based on the PC algorithm customized on the phenomenon knowledge. In particular, the combination of *Hc*, *Hl*, and *crr* provides the equivalent soil profile class by introducing the normed error as the first control factor. The geological susceptibility is separately considered; therefore, the distance from the riverbed is considered and modeled as an independent variable. On the right side of the net, the epicentral distance and Arias Intensity can be observed; the net learned both a dependency among each other and liquefaction ground evidence. Conditional and prior probabilities are specified and, in turn, employed to perform belief updating and extract posterior beliefs. The quality measure can be judged with several criteria like the Bayesian approach or minimum description length (Bouckaert et al., 2011). The score of the whole network can be decomposed as the sum (or product) of individual node scores in a way that enables local scoring and searching methods. The performance of each algorithm is summarized in Table 1 that shows the result of the 5-fold cross-validation test, which splits the whole dataset into 5 panels and estimates how the model is expected to perform when used to make predictions on data not used during the training of the model. The AUC, in conjunction with the *K* statistics, is used to rank the best learning structure. Although a perfect match exists when *K* statistics is equal to 1.0, realistically, for a site investigation on a regional scale, a *K= 0.5* match is more appropriate (Demshar, 2020).

Table 1. Summary of validation results for the above defined Bayesian networks.

	SCORE			
BBN	AUC	K-stat.	OSR	PRECISION
PC	0.81	0.442	0.72	0.70
Naïve Bayes	0.79	0.431	0.72	0.72
ANB	0.77	0.458	0.73	0.71
TAN	0.82	0.447	0.72	0.71
BS	0.81	0.421	0.72	0.56
GTT	0.81	0.460	0.73	0.69
Expert-guided*	0.81	0.461	0.73	0.70

* Ranked as the best structure because of the highest K-statistics and the physical accounting of cause-effect relationships governing the liquefaction phenomenon.

Once the general performance is evaluated through the AUC, the features of the Christchurch critical layer have been searched by setting the evidence of liquefaction and discarding those profiles not ascribable to the three-layered model (Paolella et al., 2020). It is found that, for the considered seismic scenarios, the critical layer for liquefaction is shallow ($Hc < 3m$ in 60% of cases), mid-size to large ($Hl > 3m$ in 81% of cases) and can be modeled with a $crr < 0.30$ (93%of cases) (Figure 4).

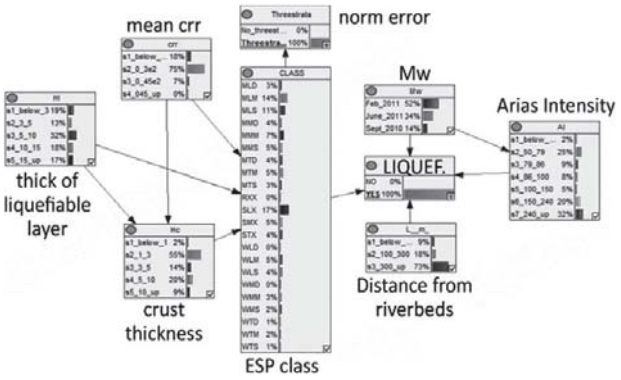

Figure 4. Back analysis of Christchurch earthquake scenarios with the selected expert-guided net.

3.4 *A probabilistic model for liquefaction triggering analysis*

The automated processing of such a number of CPT data and the availability of post-event damage surveys provides a unique chance to test the performance of current criteria and develop new models. About the latter task, the probability of observing liquefaction given the critical layer has been better investigated by splitting the liquefiable thickness range into three classes, *i.e.* $3 < Hl \leq 5m$, $5 < Hl \leq 10m$, $10 < Hl \leq 15m$ curves have been derived on these configurations. A fragility curve like the one shown in Equation 4 evaluates the probability of observing liquefaction given an intensity measure (IM) idealized by a typical lognormal distribution:

$$p(L|IM) = \phi\left(\frac{LN\left(\frac{IM_i}{\mathrm{IM_m}}\right)}{\beta}\right) \tag{4}$$

where ϕ denotes the Gaussian cumulative distribution function, IM_m is the median distribution and β is the logarithmic standard deviation. Even though that minor literature exists about the modeling of soil liquefaction vulnerability with this approach (Geyin and Maurer, 2020), fragility curves are generally adopted in procedures to assess seismic and liquefaction risk on buildings (Fotopoulou et al., 2018), road and embankments (Syner-G, 2013) and pipelines (Liu et al., 2015; Baris et al., 2020). Fragility functions are developed as an extension of deterministic models, allowing practitioners to make previsions linked to probabilistic seismic hazard analyses. After the experience of Baker (2013) in structural modelling, the maximum likelihood method is here applied to reach the appropriate data fitting. Assuming that the number of liquefaction/no liquefaction observations from each experiment is independent of observations from other experiments, the probability of observing z_j liquefaction occurrence in nj motions having $IM = x_j$ is provided by the binomial distribution (Equation 5).

$$P\left(z_j \text{ evidence in } n_j \text{ experiments}\right) = \binom{n_j}{z_j} p_j^{z_j}\left(1-p_j\right)^{n_j - z_j} \tag{5}$$

where p_j is the probability that a ground motion with $IM = x_j$ will trigger liquefaction. The maximum likelihood is thus implemented to find the fragility function capable of predicting p_j with the highest probability of fitting experimental data. When analysis data are obtained at multiple IM levels, we take the product of the binomial probabilities (from Equation 5) at each IM level to obtain the likelihood for the entire data set.

$$Likelihood = \prod_{J=1}^{m} \binom{n_j}{z_j} p_j^{z_j}\left(1-p_j\right)^{n_j - z_j} \tag{6}$$

where m is the number of IM levels and Π is a product over all levels.

The pairs of IM_m and β obtained for each soil configuration by maximizing Equation 6 are reported in Table 2; in addition, the maximum observed value of

arias intensity is indicated, meaning that discretion should be used in using the obtained fragility functions out from the suggested range. Figure 5 displays both the suit of functions showed in Table 2 and the interpolated experimental points; a graphical comparison among each other is presented in Figure 5d. It reflects the positive correlation between thick of liquefiable layer *Hl* and liquefaction occurrence for a given shaking.

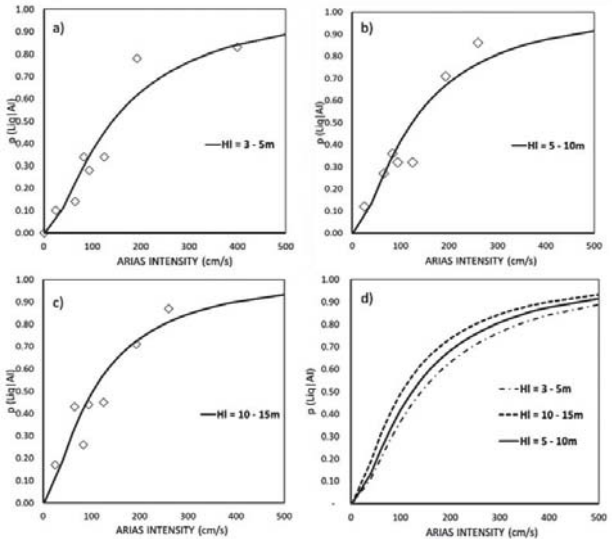

Figure 5. Probability of observing liquefaction manifestations given the AI, for each profile configuration: a) $3 < Hl \leq 5m$; b) $5 < Hl \leq 10m$; c) $10 < Hl \leq 15m$; d) general comparison.

Table 2. Summary of fragility function parameters.

H1(m)	IMm	β	Arias Intensity (cm/s) range
3-5	142.3	1.03	< 350
5-10	123.8	1.02	< 350
10-15	102.6	1.06	< 350

4 CONCLUSIONS

After processing ≈30′000 CPTs, seven structures of Bayesian Networks are tested against the liquefaction ground evidence induced by three main shocks of the 2010 – 2011 Christchurch Earthquake Sequence. The validation criteria ranked the "expert-guided" Net as the best architecture. It accounts for the cause-effect relationships ruling the phenomenon introducing new variables that better describe the geological/geotechnical susceptibility (e.g., epicentral and riverbeds distances) not considered by traditional liquefaction severity indicators. The robustness of the proposed method herein is quantified by an AUC equal to 0.81, *i.e.*, ≈15% higher than traditional indices, which cannot manage all the uncertainties connected with the randomness of seismic source, spatial variability, and error propagation (Paolella et al., 2020). The Bayesian Network-based back analysis located the Christchurch critical sandy layer at a relatively small depth ($Hc < 3m$), and a very low relative density is found on it ($crr < 0.3$). The following analysis defined a set of soil fragility curves that couple the liquefaction susceptibility of such a critical layer to the seismicity of the area via the Arias Intensity measure. Their applicability should respect the Arias Intensity range reported in Table 2, requiring additional analyses and judgment if this value is exceeded.

REFERENCES

Arias A., 1970: "A measure of earthquake intensity". Seismic design for nuclear power plants, R. J. Hansen, ed., MIT Press, Cambridge, Mass.

Baker J. W., 2013: "Efficient analytical fragility function fitting using dynamic structural analysis", Earthquake Spectra.

Baris A., Spacagna R. L., Paolella L., Koseki J. & Modoni G., 2020: "Liquefaction fragility of sewer pipes derived from the case study of Urayasu (Japan)". Bulletin of Earthquake Engineering, Springer B.V. 2020.

Bird, J., Crowley, H., Pinho, R., Bommer, J.; 2005: "Assessment of building response to liquefaction induced differential ground deformation". Bulletin of the New Zealand Society for Earthquake Engineering, 38-4, Dec. 2005, 215–234.

Bouckaert R.R., 2011: "WEKA Manual for version 3-7-5".

Cheng, J., David A. B. & Weiru L., 1997: "An Algorithm for Bayesian Belief Network Construction from Data". Proceedings of AI & Statistics, pages 83-90.

Cornell, C.A., and Krawinkler, H. 2000. "Progress and Challenges in Seismic Performance Assessment". PEER Center News, 3, 1–3.

Ching J., Phoon K.K., 2017: "Characterizing uncertain site-specific trend function by sparse Bayesian learning". ASCE Journal of Engineering Mechanics, 143(7), 04017028.

Cooper G. F., and Herskovits E. A., 1992: "A Bayesian method for the induction of probabilistic networks from data". Machine Learning, 9:309–347.

Cubrinovski M., 2013: "Liquefaction-Induced Damage in the 2010-2011 Christchurch (New Zealand) Earthquakes". In: Proceedings of the 7th International Conference on Case Histories in Geotechnical Engineering, 29 Apr–4 May, Chicago, Illinois.

Demshar J., 2020: "Development of Liquefaction Hazard Map Using a Geostatistical Method". University of Minnesota, ProQuest LLC.

Fotopoulou S., Karafagka S., Pitilakis K., 2018, Vulnerability assessment of low-code reinforced concrete frame buildings subjected to liquefaction-induced differential displacements, Soil Dynamics and Earthquake Engineering 110 (2018) 173–184.

GeNIe, (2020). BayesFusion, LLC. Retrieved from http://www.bayesfusion.com/.

Geyn M., and Maurer B. W., 2020: "Fragility functions for liquefaction-induced ground failure". Journal of Geotechnical and Geoenvironmental Engineering, © ASCE, ISSN 1090-0241.

Hu, J., Tang, X., and Qiu, J.: Assessment of Seismic liquefaction potential based on Bayesian network constructed

from domain knowledge and history data, Soil Dyn. Earthq. Eng., 89, 49–60, 2016.

Liu M., Giovinazzi S. and Lee P., 2015: "Seismic fragility functions for sewerage pipelines". (ASCE), Pipelines Conference 2015, 23-26 August, Baltimore (MD), USA.

Lusted L.B., 1971, Signal detectability and medical decision making. Science 171: 1217–1219.

Millen M., Viana da Fonseca A., Quintero J., Ferreira C., Oztoprak S., Bozbey I., Oser C., Aysal N., Kosic M., Logar J., 2020: "Equivalent soil profiles to integrate in situ tests results and soil-structure interaction in liquefiable soils. The Adapazari case-study". Bull Earthq Eng (Special issue).

Paolella L., Salvatore E., Spacagna R. L., Modoni G., Ochmanski M., 2019: "Prediction of Liquefaction Damage with Artificial Neural Networks", Atti 7ICEGE 2019.

Paolella L., Spacagna R. L., Chiaro G., Modoni G., 2020: "A simplified vulnerability model for the extensive liquefaction risk assessment of buildings". Bullettin of Earthquake Engineering, 2020.

Pearl J., 1988: "Probabilistic Reasoning in Intelligent Systems: Networks of Plausible Inference". San Francisco, California: Morgan Kaufmann Publishers, Inc.

Spacagna R.L., Porchia A., Fabozzi S., Cesarano M., Peronace E., Romagnoli G., 2021: Seismic liquefaction assessment in Calabria region in Southern Italy: a geostatistical approach at regional and sub-regional scale. International Journal of Geosciences (accepted).

Spirtes P., Glymour c., and R. Scheines. 1993: "Causation, Prediction and Search". Springer Verlag, Berlin.

SYNER-G, 2013: "Systemic Seismic Vulnerability and Risk Analysis for Buildings, Lifeline Net-works and Infrastructures Safety Gain". ISBN: 978-92-79-33135-0. DOI: 10.2788/23242. Web-site: http://www.vce.at/SYNER-G/files/project/proj-overview.html

Tang X., Bai X., Hu J. H., Qiu J., 2018: "Assessment of liquefaction-induced hazards using Bayesian networks based on standard penetration test data". Natural Hazards and Earth System Sciences 18(5):1451–1468.

Tesfamariam S., 2013: "Seismic risk analysis using Bayesian belief networks". In Handbook of seismic risk analysis and management of civil infrastructure systems, S. Tesfamariam and K. Goda editors, Woodhead Publishing Limited, pp.175–208.

Tonkin & Taylor, Ltd. (2013): "Liquefaction Vulnerability Study". Report to Earthquake Commission. Tand T ref. 52020.0200/v1.0, prepared by S. van Ballegooy and P. Malan, available at https://canterburygeotechnical database.projectorbit.com.

van Ballegooy S., Malan P., Lacrosse V., Jacka M.E., Cubrinovski M., Bray J.D., O'Rourke T.D., Crawford S. A., Cowan H., 2014: "Assessment of Liquefaction-Induced Land Damage for Residential Christchurch". Earthquake Spectra (30) No. 1: pages 31–55, February 2014.

Witten I.H., Frank E., 2005: "Data mining: Practical Machine Learning Tools and Techniques. Burlington, MA: Elsevier pp. 143–185.